Ground-state properties of anyons in a one-dimensional lattice

2015 New J. Phys. 17 123016

(http://iopscience.iop.org/1367-2630/17/12/123016)

New Journal of Physics
The open access journal at the forefront of physics

Deutsche Physikalische Gesellschaft DPG
IOP Institute of Physics

Published in partnership with: Deutsche Physikalische Gesellschaft and the Institute of Physics

CrossMark

OPEN ACCESS

RECEIVED
10 September 2015

REVISED
14 November 2015

ACCEPTED FOR PUBLICATION
20 November 2015

PUBLISHED
14 December 2015

PAPER

Ground-state properties of anyons in a one-dimensional lattice

Guixin Tang[1,2], **Sebastian Eggert**[2] **and Axel Pelster**[2]

[1] Department of Physics, Harbin Institute of Technology, 150001 Harbin,150001 Harbin, People's Republic of China
[2] Physics Department and Research Center OPTIMAS, University of Kaiserslautern, D-67663 Kaiserslautern, Germany

E-mail: tangguixin@hit.edu.cn

Keywords: anyons, Anyon–Hubbard model, the fractional Jordan–Wigner transformation, the quasi-momentum distribution, one-dimensional lattice

Abstract

Using the Anyon–Hubbard Hamiltonian, we analyze the ground-state properties of anyons in a one-dimensional lattice. To this end we map the hopping dynamics of correlated anyons to an occupation-dependent hopping Bose–Hubbard model using the fractional Jordan–Wigner transformation. In particular, we calculate the quasi-momentum distribution of anyons, which interpolates between Bose–Einstein and Fermi–Dirac statistics. Analytically, we apply a modified Gutzwiller mean-field approach, which goes beyond a classical one by including the influence of the fractional phase of anyons within the many-body wavefunction. Numerically, we use the density-matrix renormalization group by relying on the ansatz of matrix product states. As a result it turns out that the anyonic quasi-momentum distribution reveals both a peak-shift and an asymmetry which mainly originates from the nonlocal string property. In addition, we determine the corresponding quasi-momentum distribution of the Jordan–Wigner transformed bosons, where, in contrast to the hard-core case, we also observe an asymmetry for the soft-core case, which strongly depends on the particle number density.

1. Introduction

A fundamental principle of quantum statistical mechanics in three dimensions is the existence of two types of particles: bosons obeying Bose–Einstein statistics and fermions obeying Fermi–Dirac statistics. However, in a two-dimensional electron liquid, quasi-particles made of electrons in the fractional quantum Hall effect are charged anyons obeying fractional statistics [1–5]. While exchanging two anyons, the many-body wavefunction acquires a fractional phase $e^{i\theta}$, where the statistical parameter θ varies with the interval $0 < \theta < \pi$ and corresponds to a fractional statistics. As compared to bosons and fermions, anyons exhibit a wide range of previously unexpected properties and the concept of anyons plays an important role in numerous studies of condensed matter physics and of topological quantum computation [6–13]. In order to generalize the Bose–Einstein and Fermi–Dirac statistics by allowing a maximal finite integer particle number occupying the same quantum state, Gentile supplied an intermediate statistics that had been proven to be also valid for a q-fermion [14–19]. However, Shen *et al* pointed out that the anyon statistics was not a complete analogue of the Gentile statistics [20]. Based on a generalized Pauli exclusion principle, Haldane provided a useful concept of fractional statistics in arbitrary dimensions [21]. Polychronakos also suggested another form of the fractional exclusion statistics [22]. However, it was shown via the virial expansion that all these fractional statistics proposed in the literature do not apply for anyons [20, 23].

In one-dimension (1D), anyons were realized as low-energy elementary excitations of the Hubbard model of fermions with correlated hopping processes [24]. Alternatively, it was suggested to create anyons by bosons with complex-valued occupation-dependent hopping amplitudes by photon-assisted tunneling in 1D optical lattices [25, 26]. Recently, Greschner and Santos proposed a Raman scheme to improve the proposal of Keilmann *et al* in [25] and deduced a rich ground-state physics including Mott-insulators with attractive interactions, pair-superfluids, dimer phases, and multi-critical points [27]. An even simpler scheme for realizing the physics of 1D anyons with ultracold bosons in an optical lattice has recently been proposed in [28]. It relies on lattice-shaking-induced resonant tunneling against the energy off-sets created by the combination of both a potential tilt and on-site repulsion. In contrast to the above mentioned former proposals based on internal atomic degrees of freedom, no lasers additional to those already used for the creation of the optical lattice are required [28].

The physical properties of 1D anyons are intriguing and complicated. Theoretically, using the generalized coordinate Bethe ansatz method, Kundu obtained the exact solution of a 1D anyon gas with the delta-function potential, which shows that the effective interaction among the anyons is modified by the anyonic statistical parameter [29]. Furthermore, the 1D anyon gas with a special interaction potential has been investigated in various 1D systems in order to get the ground-state properties of the 1D anyon gas [30–35]. For anyons in the 1D lattice systems one investigated, for instance, the statistically induced phase transition [25], quantum scaling properties [24], dynamics properties of hard-core anyons [36, 37], quantum walks [38, 39], and anyonic Bloch oscillations [40]. For the hard-core anyons in the 1D optical lattice, Hao *et al* investigated how the fractional statistics affected the ground-state properties by mapping the hard-core anyonic Hamiltonian to a noninteracting fermionic system with a generalized Jordan–Wigner transformation [41]. By calculating the one-particle Greens function of the ground state, the reduced one-body density matrix and, thus, the quasi-momentum distributions can be obtained for different statistical parameters of anyons. The results showed that the momentum distributions in the Bose and Fermi limit turned out to be symmetric, but those of anyons were in general asymmetric and shifted due to the fractional statistics that anyons obey.

In this paper we complement the previous studies of the ground-state properties of a 1D quantum gas of anyons confined in optical lattices. To this end we map the Anyon–Hubbard (AH) model to an occupation-dependent hopping Bose–Hubbard model with the help of a fractional version of the Jordan–Wigner transformation. This mapping has the consequence that the Hilbert space of anyons can be constructed from that of bosons, so that one has access to the two-point correlation function of either the original anyonic or the Jordan–Wigner transformed bosonic creation and annihilation operators. With this we investigate the quasi-momentum distributions of either bosons or anyons, the latter interpolating between Bose–Einstein statistics and Fermi–Dirac statistics. Firstly, in the hard-core limit, we determine the quasi-momentum distributions of anyons with density-matrix renormalization group (DMRG) calculations, which numerically reproduces the results of Hao *et al* [41]. In addition, by suggesting a modified Gutzwiller mean-field approach to include the influence of the fractional phase of anyons within the many-body wavefunction, we obtain an approximative analytic expression for the numerical results of [41] both for a finite system and in the thermodynamic limit. In particular, we analyze in detail how peak-shift and asymmetry of the quasi-momentum distribution of anyons depend on both the fractional phase θ and the particle number density n_0. Furthermore, we extend the findings of [41] by working out also the more general soft-core case. The quasi-momentum distribution of anyons reveals the pseudofermion property at the fractional phase $\theta = \pi$. Surprisingly, the quasi-momentum distributions of the Jordan–Wigner transformed bosons shows a density-dependent asymmetry which is not found for the hard-core case.

The outline of this paper is as follows: in section 2 the AH model and the mapping between anyons and bosons are discussed. Both the classical and the modified Gutzwiller mean-field approach is introduced in section 3. The ground-state properties of the 1D AH model are determined by studying the quasi-momentum distribution of anyons and bosons in both the hard-core and the soft-core case in sections 4 and 5 respectively. Conclusions are given in section 6.

2. AH model

The hopping dynamics of correlated anyons on a 1D lattice is described by the AH Hamiltonian [25]

$$\hat{H}^a = -J\sum_{j=1}^{L}\left(\hat{a}_j^\dagger \hat{a}_{j+1} + \text{h.c.}\right) + \frac{U}{2}\sum_{j=1}^{L}\hat{n}_j\left(\hat{n}_j - 1\right), \tag{1}$$

where $J > 0$ denotes the tunneling amplitude connecting two neighboring sites, U stands for the on-site interaction energy, $\hat{n}_j = \hat{a}_j^\dagger \hat{a}_j$ represents the number operator at site j, and the operators $\hat{a}_j^\dagger$, $\hat{a}_j$ create or annihilate an anyon on site j. For 1D anyons, the operators $\hat{a}_j^\dagger$ and $\hat{a}_j$ obey the generalized commutation relations [25, 29]

$$\begin{aligned} \hat{a}_j\hat{a}_k^\dagger - \mathrm{e}^{-\mathrm{i}\theta\,\mathrm{sgn}(j-k)}\hat{a}_k^\dagger\hat{a}_j &= \delta_{jk}, \\ \hat{a}_j\hat{a}_k - \mathrm{e}^{\mathrm{i}\theta\,\mathrm{sgn}(j-k)}\hat{a}_k\hat{a}_j &= 0, \end{aligned} \tag{2}$$

where θ is the statistical exchange phase, the sign function $\mathrm{sgn}(j-k) = -1,\ 0,\ +1$ for $j < k, j = k$, and $j > k$, respectively. Note that, since the sign function $\mathrm{sgn}(j-k) = 0$ for $j = k$, two particles on the same site behave as ordinary bosons irrespective of the statistical parameter θ. Moreover, anyons with the statistical exchange phase $\theta = \pi$ are pseudofermions, i.e. while being bosons on-site, they are fermions off-site.

Here we use an exact Anyon–Boson mapping in 1D in terms of a fractional version of the Jordan–Wigner transformation [25]

$$\hat{a}_j = \hat{b}_j \exp\left(\mathrm{i}\theta \sum_{i=1}^{j-1} \hat{n}_i\right), \tag{3}$$

where the number operator reads $\hat{n}_i = \hat{a}_i^\dagger \hat{a}_i = \hat{b}_i^\dagger \hat{b}_i$ and $\hat{b}_i, \hat{b}_i^\dagger$ are bosons operators following the commutation relation $[\hat{b}_i, \hat{b}_j^\dagger] = \delta_{ij}$ and $[\hat{b}_i^\dagger, \hat{b}_j^\dagger] = 0 = [\hat{b}_i, \hat{b}_j]$. Inserting the Anyon–Boson mapping (3) into equation (1), the Hamiltonian $\hat{H}^a$ can be rewritten as [25]

$$\hat{H}^b = -J\sum_{j=1}^{L}\left(\hat{b}_j^\dagger \hat{b}_{j+1} \mathrm{e}^{\mathrm{i}\theta \hat{n}_j} + \mathrm{h.c.}\right) + \frac{U}{2}\sum_{j=1}^{L} \hat{n}_j\left(\hat{n}_j - 1\right), \tag{4}$$

where the conditional hopping of bosons from right to left, i.e. $j + 1 \to j$, occurs with an occupation-dependent amplitude $J\mathrm{e}^{\mathrm{i}\theta\hat{n}_j}$. If the target site j is unoccupied, the hopping amplitude is simply J. If it is occupied by one boson, the amplitude becomes complex and reads $J\mathrm{e}^{\mathrm{i}\theta}$, and so on. We emphasize that the hard-core limit of anyons in equation (1) coincides with that of bosons in equation (4) due to $\hat{n}_i = \hat{a}_i^\dagger \hat{a}_i = \hat{b}_i^\dagger \hat{b}_i$. It is also clear that the mapped bosonic Hamiltonian (4) describes local occupation numbers beyond the hard-core limit $n_j > 1$.

Using the nonlocal exact mapping (3) between anyons and bosons, the AH Hamiltonian (1) leads to a bosonic Hamiltonian equation (4) that can be solved either analytically or numerically in order to determine the ground-state properties of anyons in 1D lattice systems. Theoretically, since the reflection parity symmetry in the Hamiltonian is broken, we suggest below a modified Gutzwiller mean-field, which goes beyond the classical one found in literature [42–45] in order to include the influence of the fractional phase of anyons on the hopping dynamics. To get numerical results, we use the DMRG [46–50], which was already applied to the realm of anyons, for instance, in [25]. To this end, we rely on the ansatz of matrix product states (MPSs) with the system length L and open boundary conditions, which is more efficient than periodic boundaries [51–55]. The code is based on a variational ansatz using MPS with the restricted subspace of integer filling, where our simulations admit a maximum of five particles per site and the maximum bond dimension of MPS equals to 1000 [56]. Moreover, [53, 54, 56] show the respective details how to calculate the expectation of the string operator in equation (3) and the correlation functions in DMRG with MPS ansatz.

3. Mean-field approximation

At first we work out a Gutzwiller mean-field approach, which turns out to provide qualitative satisfactory results for the quasi-momentum distributions. In a Gutzwiller (GW) approach for bosons, the many-particle state $|G\rangle$ is generically approximated by a product state of single lattice-site states $|\Phi_j\rangle$, which can be expressed as a superposition of different number states on a lattice site [45]

$$|G\rangle = \prod_j \left|\Phi_j\right\rangle = \prod_j \left(\sum_{n=0}^{n_{\max}} f_n^{(j)}\ |n\rangle\right). \tag{5}$$

Here $n_{\max}$ represents a truncation at some sufficiently large maximal particle number and $f_n^{(j)}$ denotes the Gutzwiller probability amplitude of finding n bosons on site j, which is normalized such that

$$\sum_{n=0}^{n_{\max}} \left|f_n^{(j)}\right|^2 = 1. \tag{6}$$

The total energy of the system

$$\mathcal{E}_{\mathrm{tot}} = \mathcal{E}_{\mathrm{int}} + \mathcal{E}_{\mu} + \mathcal{E}_{\mathrm{kin}} \tag{7}$$

then follows from determining the ground-state expectation values of the respective operators according to the appendix. As a consequence, the interaction energy (A.1), the chemical potential term (A.2), and the kinetic energy (A.3) depend on the Gutzwiller coefficients $f_n^{(j)}$. Due to the polar decomposition $f_n^{(j)} = F_n^{(j)}\mathrm{e}^{\mathrm{i}\alpha_n^{(j)}}$, the total energy (7) has to be minimized with respect to both the absolute values $F_n^{(j)}$ and the phases $\alpha_n^{(j)}$.

In the classical GW mean-field approach of a homogeneous system, to which we refer as cGW in the following, one assumes that the ground state is a product of identical states on each of the L lattice sites [42–45], i.e.

$$\left|\Phi_j\right\rangle = |\Phi\rangle, \quad f_n^{(j)} = f_n. \tag{8}$$

This has the consequence

$$F_n^{(j)} = F_n, \quad \alpha_n^{(j)} = \alpha_n, \tag{9}$$

i.e. one has the identical wave function on each lattice site.

Due to the occupation-dependent amplitude $J\mathrm{e}^{\mathrm{i}\theta\hat{n}_j}$ for nearest-neighbor hopping in the bosonic Hamiltonian (4), the reflection parity symmetry is broken. Therefore, we suggest to drop the cGW constraint of having identical states on each site to a modified GW mean-field approach (mGW). To this end, we note that the kinetic energy equation (A.5) in the appendix depends on the difference $\beta_n^{(j)} \equiv \alpha_n^{(j)} - \alpha_{n+1}^{(j)}$ of the phases of the probability amplitudes $f_n^{(j)}$ and $f_{n+1}^{(j)}$ of finding n and $n+1$ bosons on site j, respectively. If all phase differences would be identical, we would recover cGW. Therefore, we define mGW according to

$$F_n^{(j)} = F_n, \quad \Delta\beta_n^{(j)} = \beta_n^{(j)} - \beta_n^{(j+1)} \equiv \Delta\beta_n. \tag{10}$$

In order to fix the values of the phase differences $\beta_n^{(j)}$, we complement (10) by the additional assumption

$$\beta_n^{(j)} + \beta_n^{(j+1)} \equiv 2\beta_n. \tag{11}$$

This means that the absolute value $F_n^{(j)}$ of the probability amplitude $f_n^{(j)}$ is identical on each site and the non-vanishing phase difference $\Delta\beta_n^{(j)}$ between two nearest-neighbor sites is the same in the whole chain.

The application of cGW and mGW is performed in the appendix for both the hard-core case in section A.1, which means $n_{\max} = 1$, and the soft-core case by assuming $n_{\max} = 2$ in section A.2. Provided that Gutzwiller amplitudes and phases have been determined, one can calculate the two-point correlation function of bosons, which has the rather simple expression

$$\langle \hat{b}_i^\dagger \hat{b}_j \rangle = \delta_{ij}\langle \hat{n}_i \rangle + \left(1 - \delta_{ij}\right)\langle \hat{b}_i^\dagger \rangle \langle \hat{b}_j \rangle. \tag{12}$$

The correlation function of anyons can be written as

$$\langle \hat{a}_i^\dagger \hat{a}_j \rangle \overset{i<j}{\rightarrow} \left\langle \hat{b}_i^\dagger \mathrm{e}^{\mathrm{i}\theta\hat{n}_i} \right\rangle \left(\prod_{i<l<j} \left\langle \mathrm{e}^{\mathrm{i}\theta\hat{n}_l} \right\rangle \right) \langle \hat{b}_j \rangle, \tag{13a}$$

$$\langle \hat{a}_i^\dagger \hat{a}_j \rangle \overset{i>j}{\rightarrow} \langle \mathrm{e}^{-\mathrm{i}\theta\hat{n}_j} \hat{b}_j \rangle \left(\prod_{j<l<i} \left\langle \mathrm{e}^{-\mathrm{i}\theta\hat{n}_l} \right\rangle \right) \langle \hat{b}_i^\dagger \rangle, \tag{13b}$$

$$\langle \hat{a}_i^\dagger \hat{a}_j \rangle \overset{i=j}{\rightarrow} \langle \hat{n}_j \rangle, \tag{13c}$$

where the respective expectation values depend on the Gutzwiller amplitudes $f_n^{(j)}$ according to equation (A.4a) in the appendix.

Furthermore, in order to investigate the effect of the anyon statistical parameter θ, we will focus on density distributions of bosons and anyons in the quasi-momentum space, which are defined via the Fourier transformation of the correlation function

$$\langle \hat{n}_k^{(\mathrm{b})} \rangle = \frac{1}{L}\sum_{ij} \mathrm{e}^{\mathrm{i}k\left(x_i - x_j\right)} \langle \hat{b}_i^\dagger \hat{b}_j \rangle, \tag{14a}$$

$$\langle \hat{n}_k^{(\mathrm{a})} \rangle = \frac{1}{L}\sum_{ij} \mathrm{e}^{\mathrm{i}k\left(x_i - x_j\right)} \langle \hat{a}_i^\dagger \hat{a}_j \rangle. \tag{14b}$$

Provided that anyons are simulated by an occupation-dependent hopping of bosons according to the proposals in [25–28], the bosonic correlation function (14a) should be measurable in time-of-flight experiments. In those experiments it is unclear whether the corresponding anyonic correlation function (14b) is also observable, however, for comparison, a deeper understanding, and possible future applications it is worth while to determine the θ-dependence of $\langle \hat{n}_k^{(\mathrm{a})} \rangle$ in the following.

At first, we are going to find the ground state of a homogeneous system for a given particle number density $n_0 > 0$, ratio J/U, and varying statistical parameter θ. Thus, combining the analytic approaches cGW, mGW with numerical results from DMRG, we determine the correlation functions and, thus, investigate the quasi-momentum distributions of the ground state.

4. Hard-core anyons

In order to illustrate the applicability of the Gutzwiller mean-field theory, we investigate at first the simplest case of hard-core anyons. This means that we assume $U/J \to \infty$, where bosons are impenetrable and each site contains at most one particle, i.e., $n_{\max} = 1$. In the following, we present only the calculations of the correlation

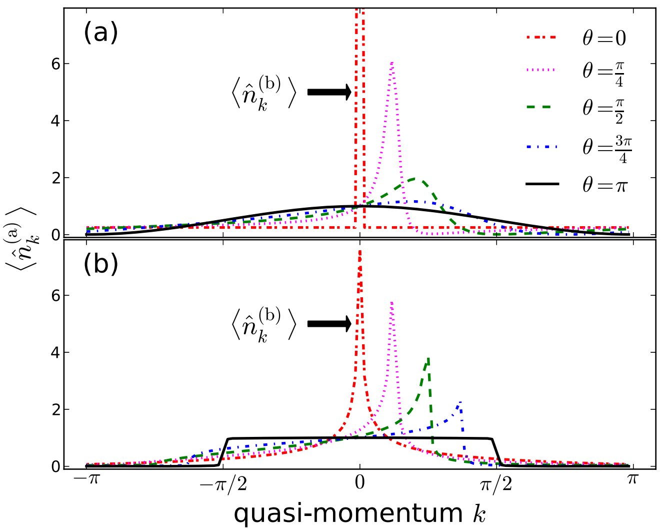

Figure 1. Quasi-momentum distribution of the ground state in a hard-core system ($n_0 = N/L = 0.5, L = 120$). (a) Gutzwiller approach and (b) DMRG for anyons and bosons.

function and the quasi-momentum distribution, while the mathematical details for minimizing the total energy are relegated to section A.1 of the appendix.

According to equation (12), the correlation function of bosons reads

$$\langle\hat{b}_i^\dagger\hat{b}_j\rangle = \delta_{ij}n_0 + \left(1 - \delta_{ij}\right)n_0\left(1 - n_0\right)\mathrm{e}^{\mathrm{i}\left(\beta_0^{(i)} - \beta_0^{(j)}\right)}, \tag{15}$$

which reduces to

$$\langle\hat{b}_i^\dagger\hat{b}_j\rangle = \delta_{ij}n_0^2 + n_0\left(1 - n_0\right), \tag{16}$$

since $\Delta\beta_0 = \beta_0^{(j)} - \beta_0^{(j+1)} = 2m\pi$ (see section A.1). Using equation (14*a*), the ground-state quasi-momentum distribution of bosons can be written as

$$\langle\hat{n}_k^{(b)}\rangle = n_0^2 + n_0\left(1 - n_0\right)L\delta_{k,0}, \tag{17}$$

which is θ-independent and the number of particles in the condensate is $N_0 = N(1 - n_0)$. Figure 1 shows the resulting ground-state quasi-momentum distribution in a hard-core system at density $n_0 = 0.5$.

Since $\langle\hat{n}_k^{(b)}\rangle$ in equation (17) is θ-independent in the GW approach, if one changes θ from 0 to π, all quasi-momentum distributions with different θ coincide as shown in figure 1(a). The quasi-momentum distribution of bosons $\langle\hat{n}_k^{(b)}\rangle$ in DMRG as shown in figure 1(b) turns out to be also θ-independent because the phase factor disappears in the bosonic Hamiltonian (4) in the hard-core limit and the systems reduces to a hard-core Bose–Hubbard model. As a consequence, bosons condense at zero quasi-momentum in both the GW approach and DMRG. However, the bosonic population $N(1 - n_0)$ of $k = 0$ in the GW approach is much larger than that in DMRG because the mean-field approach does not contain quantum fluctuations which generally broaden the quasi-momentum distributions.

In the Bose limit $\theta = 0$, we have $\hat{a}_j = \hat{b}_j$ and $\langle\hat{a}_i^\dagger\hat{a}_j\rangle = \langle\hat{b}_i^\dagger\hat{b}_j\rangle$, thus

$$\langle\hat{n}_k^{(a)}(\theta = 0)\rangle = \langle\hat{n}_k^{(b)}\rangle. \tag{18}$$

which is shown in figures 1(a) and (b) for the density $n_0 = 0.5$.

According to equations (13) and (A.4*d*) in the appendix, the correlation function of anyons reduces to

$$\langle\hat{a}_i^\dagger\hat{a}_j\rangle \overset{i<j}{\rightarrow} n_0\left(1 - n_0\right)\prod_{i<l<j}\left[\left(1 - n_0\right) + n_0\mathrm{e}^{\mathrm{i}\theta}\right], \tag{19a}$$

$$\langle\hat{a}_i^\dagger\hat{a}_j\rangle \overset{i>j}{\rightarrow} n_0\left(1 - n_0\right)\prod_{j<l<i}\left[\left(1 - n_0\right) + n_0\mathrm{e}^{-\mathrm{i}\theta}\right]. \tag{19b}$$

Using equation (14*b*), the ground-state quasi-momentum distribution of anyons can be written in the θ-dependent form for a finite open system

$$\langle \hat{n}_k^{(a)} \rangle = n_0 + n_0\left(1 - n_0\right)\frac{1}{L}\left\{(L-1)\left(e^{-ik} + e^{ik}\right) + \sum_{m=2}^{L-1}(L-m)\left[e^{-ikm}z^{m-1} + e^{ikm}z^{*m-1}\right]\right\}, \tag{20}$$

where $z = re^{i\varphi} = x + iy \equiv (1 - n_0) + n_0 e^{i\theta}$, thus $r = 1$ if $\theta = 0$ or $n_0 = 1$, otherwise $r < 1$. In the Fermi limit $\theta = \pi$, we obtain from (20)

$$\langle \hat{n}_k^{(f)} \rangle = n_0 + 2n_0\left(1 - n_0\right)\left\{\frac{\cos(k) - x}{1 - 2x\cos(k) + x^2} - \frac{\left(1 - x^L\right)\left[\cos(k)\left(1 + x^2\right) - 2x\right]}{L\left[1 - 2x\cos(k) + x^2\right]}\right\}, \tag{21}$$

where $\langle \hat{n}_k^{(f)} \rangle \equiv \langle \hat{n}_k^{(a)}(\theta = \pi) \rangle$, $x \equiv 1 - 2n_0 \in (-1, +1)$ if $0 < n_0 < 1$. In the thermodynamic limit, this reduces to

$$\langle \hat{n}_k^{(f)} \rangle \underset{|x|<1}{\overset{L\to\infty}{\longrightarrow}} n_0 + 2n_0\left(1 - n_0\right)\frac{\cos(k) - x}{1 - 2x\cos(k) + x^2}. \tag{22}$$

For the system at $n_0 = 0.5$, the GW approach gives

$$\begin{aligned} \langle \hat{n}_k^{(f)} \rangle &= 0.5 + 0.5\left(1 - \frac{1}{L}\right)\cos(k) \\ \overset{L\to\infty}{\longrightarrow} \langle \hat{n}_k^{(f)} \rangle &= 0.5 + 0.5\cos(k), \end{aligned} \tag{23}$$

which is shown as the black solid line in figure 1(a). However, in figure 1(b) from DMRG, the quasi-momentum distribution of anyons in the Fermi limit represents a step-like distribution, which is the characteristic feature of free fermions. This shows that DMRG can grasp the fermion-like feature of anyons with statistics $\theta = \pi$, whereas the GW approach achieves this only approximately.

If $K_{\max}^{(a,b)}$ defines the quasi-momentum, where $\langle \hat{n}_k^{(a,b)} \rangle$ has its maximum, we have $K_{\max}^{(a)}(\theta = 0) = 0$ and $K_{\max}^{(a)}(\theta = \pi) = 0$, i.e., both the quasi-momentum distribution of the Bose and of the Fermi limit are symmetric about zero quasi-momentum. Indeed this results from $\delta_{k,0}$ in equations (17) and (18) in the Bose limit and from calculating $\partial\langle \hat{n}_k^{(f)} \rangle / \partial k = 0$ of equations (22) and (23) in the Fermi limit.

In the fractional phase interpolating between the Bose and Fermi limit $0 < \theta < \pi$, we find from (20)

$$\langle \hat{n}_k^{(a)} \rangle = n_0 + \frac{n_0\left(1 - n_0\right)}{L}\left[\frac{(L-1) - L\left(ze^{-ik}\right) + \left(ze^{-ik}\right)^L}{e^{ik}\left(1 - ze^{-ik}\right)^2} + \text{c.c.}\right]. \tag{24}$$

In the thermodynamic limit, this reduces to

$$\langle \hat{n}_k^{(a)} \rangle \underset{r<1}{\overset{L\to\infty}{\longrightarrow}} n_0 + 2n_0\left(1 - n_0\right)\frac{\cos(k) - r\cos(\varphi)}{1 - 2r\cos(k - \varphi) + r^2}, \tag{25}$$

where $r = |1 - n_0 + n_0 e^{i\theta}|$ and $\varphi = \arg(1 - n_0 + n_0 e^{i\theta})$. Figure 1 clearly show that: (i) the respective peak of the quasi-momentum distribution is shifted to positive momentum, (ii) the quasi-momentum distribution is asymmetric about its own peak, and (iii) the quasi-momentum distributions broaden and flatten with increasing θ. Comparing figure 1(a) with (b) or $\langle \hat{b}_i^\dagger \hat{b}_j \rangle$ in equation (16) with $\langle \hat{a}_i^\dagger \hat{a}_j \rangle$ in equation (19), we conclude that the nonlocal string property of anyons, which is denoted by $\prod_{i<l<j}\left[(1 - n_0) + n_0 e^{i\theta}\right]$ or $\prod_{j<l<i}\left[(1 - n_0) + n_0 e^{-i\theta}\right]$ in equation (19), is the reason why anyons prefer to appear on positive momentum. This is explained numerically in [41].

In order to find the maximum $K_{\max}^{(a)}$ of the quasi-momentum distribution, we analytically evaluate $\partial\langle \hat{n}_k^{(a)} \rangle / \partial k = 0$ for equation (25), which gives

$$K_{\max}^{(a)} = \begin{cases} \pi - \mathcal{K}, & n_0 \geqslant 2\left(\sqrt{2} - 1\right) \text{ and } \vartheta_1 \leqslant \theta \leqslant \vartheta_2, \\ \mathcal{K}, & \text{Otherwise}, \end{cases} \tag{26}$$

where we have introduced the abbreviations

$$\vartheta_1 = \frac{\pi}{4} + \arcsin\left(\frac{2 - n_0}{\sqrt{2}\,n_0}\right),\quad \vartheta_2 = \frac{3\pi}{2} - \vartheta_1, \tag{27}$$

$$\mathcal{K} = \arcsin\frac{\sin\theta\left(2n_0 - n_0^2\right) + n_0^2\sin\theta\cos\theta}{(1 - \cos\theta)\left(1 - n_0\right)^2 + (1 + \cos\theta)}. \tag{28}$$

Figure 2(a) shows the resulting fractional phase θ-dependence of anyonic $K_{\max}^{(a)}$ at density $n_0 = 0.75, 0.5$, and 0.25. The DMRG results ($L = 120$) clearly show that the peaks of the quasi-momentum distributions increase linearly from $K_{\max}^{(a)}(\theta = 0) = 0$ (bosons) and come back to $K_{\max}^{(a)}(\theta = \pi) = 0$ (fermions) while

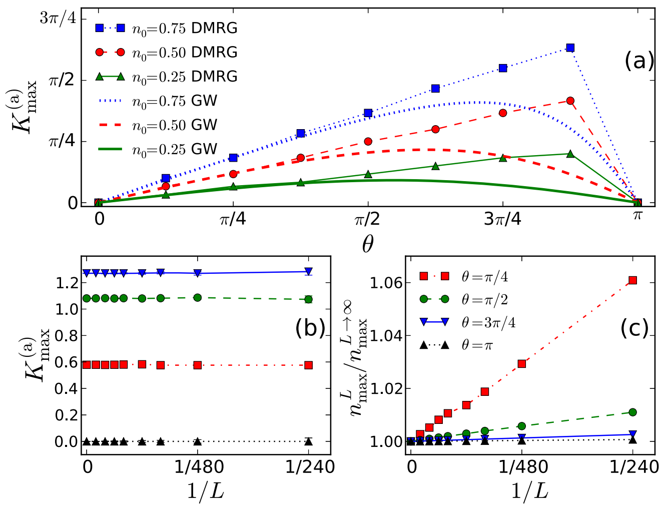

Figure 2. (a) Maximum $K_{\rm max}^{\rm (a)}$ of quasi-momentum $\langle \hat{n}_k^{\rm (a)} \rangle$ plotted against the fractional phase θ of anyons at density n_0 resulting from DMRG ($L = 120$) and GW in the thermodynamic limit $L \to \infty$. (b) $K_{\rm max}^{\rm (a)}$ plotted against the inverse system size at density $n_0 = 0.75$ resulting from GW. (c) Maximum $\langle \hat{n}_k^{\rm (a)} \rangle$ of the finite system size L divided by that of the infinite system size $L \to \infty$ plotted against the inverse system size at density $n_0 = 0.75$ resulting from GW.

increasing θ. The GW approach shows the same linearly increasing property at small θ, i.e. near bosons. This can be quantitatively understood by taking the limit $\theta \to 0$ in equations (26) and (28):

$$K_{\rm max}^{(a)}(\theta \to 0) \simeq \arcsin\left(n_0\theta\right) \simeq n_0\theta. \tag{29}$$

At the Fermi side $\theta \to \pi$, we have correspondingly

$$K_{\rm max}^{\rm (a)}(\theta \to \pi) \simeq \arcsin\frac{n_0(\pi - \theta)}{1 - n_0} \simeq \frac{n_0(\pi - \theta)}{1 - n_0}, \tag{30}$$

where the slope of $K_{\rm max}^{\rm (a)}$ from GW is smaller than that from DMRG. In general, the GW approach always yields a smaller shift of positive momentum in comparison with the DMRG results for any statistical parameter of anyons between the Fermi and the Bose case. Moreover, we find that both DMRG and GW give a larger peak shift for a bigger particle number density n_0.

In order to determine the thermodynamic limit of the quasi-momentum distribution, figures 2(b) and (c) show the system size dependence of $K_{\rm max}^{\rm (a)}$ and $n_{\rm max}^{L}/n_{\rm max}^{L\to\infty}$ at density $n_0 = 0.75$ in the GW approach, where $n_{\rm max}^{L}$ is the maximum value of the quasi-momentum distribution with the finite system size L and $n_{\rm max}^{L\to\infty}$ corresponds to the thermodynamic limit. Considering the uncertainty of the quasi-momentum in the finite system $\Delta k = 2\pi/L$, $K_{\rm max}^{\rm (a)}$ turns out to be independent of the system size. According to figure 1, the bosons condense at zero momentum with a sharp distribution and the fermions have a flat distribution. In figure 2(c), with θ increasing from the Bose to the Fermi case, we find that the condensate population near the Bose side slightly depends on the system size, but the maximum particle number near the Fermi side is almost independent on the system size, since the behavior of anyons with $\theta \sim \pi$ looks much more like fermions without condensation. Note that we do not show here the case of bosons $\theta = 0$ because bosons condense at zero momentum.

5. Soft-core anyons

Before going to the soft-core case, we remind that within the Gutzwiller theory $\langle \hat{b}_i^\dagger \hat{b}_j \rangle$ and $\langle \hat{n}_k^{\rm (b)} \rangle$ in equations (16) and (17) turn out to be independent of the fractional phase θ of hard-core anyons because $\Delta\beta_0 = 2m\pi$ and the local state $|2\rangle$ is not occupied, i.e. $F_2 = 0$. Considering the occupation-dependent hopping in the soft-core case, we are going to discuss the influence of $\Delta\beta_1$ and non-vanishing F_2 in the following. The respective details of minimizing the total energy are given in section A.2 of the appendix.

5.1. Boson quasi-momentum distribution

According to equation (12) and supposing $n_{\max} = 2$, the correlation function of bosons is

$$\langle \hat{b}_i^\dagger \hat{b}_j \rangle = \delta_{ij} n_0 + \left(1 - \delta_{ij}\right)\left[A + B e^{i(i-j)\theta}\right], \tag{31}$$

where $A \equiv F_1^2(F_0^2 + \sqrt{2}F_0F_2)$, $B \equiv F_1^2(\sqrt{2}F_0F_2 + 2F_2^2)$ and $A + B = C$. Using equation (14a), the quasi-momentum distribution of bosons can be written as

$$\langle \hat{n}_k^{(b)} \rangle = n_0 - C + AL\delta_{k,0} + B\frac{1 - \cos[(k+\theta)L]}{L[1 - \cos(k+\theta)]} \tag{32}$$

and yields in the thermodynamic limit

$$\langle \hat{n}_k^{(b)} \rangle \overset{L\to\infty}{\to} n_0 - C + A\delta(k) + B\delta(k+\theta). \tag{33}$$

Here, compared with the θ-independent $\langle \hat{n}_k^{(b)} \rangle$ of the hard-core case in equation (17), the quasi-momentum distribution of bosons from mGW has a background distribution $n_0 - C$ and two peaks at $k = 0$ and $k = -\theta$ with the intensities A and B, respectively.

Noticeably, if comparing the intensity $A = F_1^2(F_0^2 + \sqrt{2}F_0F_2)$ of the $k = 0$ peak with the intensity $B = F_1^2(\sqrt{2}F_0F_2 + 2F_2^2)$ of the $k = -\theta$ peak, we find that the discrepancy between the intensities A and B is determined by the occupation F_0^2 of $|0\rangle$ and F_2^2 of $|2\rangle$. As these occupations F_0^2 and F_2^2 change with the density n_0, the resulting quasi-momentum distribution of bosons reveals a characteristic density dependency. Therefore, we discuss now different density regimes.

In the dilute limit $n_0 \ll 1$, the positive Hubbard U depresses the state $|2\rangle$ and $F_2^2 \sim 0$, thus the properties of $\langle \hat{n}_k^{(b)} \rangle$ are similar to that of the hard-core case. Figure 3(a) shows the quasi-momentum distribution of bosons at density $n_0 = 0.25$ and $J/U = 0.1$ in the mGW approach. For $\theta = 0$, we have $\langle \hat{n}_k^{(b)} \rangle = n_0 - C + C\delta(k)$, which demonstrates that there exists only one peak of the intensity $C = A + B$ at $k = 0$ and the quasi-momentum distribution is symmetric. For the case of $0 < \theta \leqslant \pi$, we have (33), which demonstrates that there exists one much lower peak of the intensity B at the negative momentum $k = -\theta$ than that of the intensity A at $k = 0$ due to $F_2^2 \ll F_0^2$. Here, we should note that $\langle \hat{n}_k^{(b)}(\theta = \pi) \rangle$, which is plotted for slightly asymmetric interval $-\pi \leqslant k < \pi$ in figure 3(a), is also a symmetric distribution since $\langle \hat{n}_k^{(b)} \rangle$ has period 2π.

The results of DMRG with the same parameters are shown in figure 3(d), where the symmetric quasi-momentum distribution of $\theta = 0$ is a little sharper than that of $\theta = \pi$. But for the case of $0 < \theta < \pi$, there exists an asymmetric quasi-momentum distribution and more bosons have negative momentum according to the inset of figure 3(d). In general, quantum fluctuations broaden $\langle \hat{n}_k^{(b)} \rangle$ from mGW. Taking this into account, if we would add the effect of quantum fluctuations on the mGW quasi-momentum distribution, the peak at $k = 0$ and $k = -\theta$ would broaden. Since the peak at $k = -\theta$ from mGW is pretty low, a broadening would be merged into the background of the quasi-momentum distribution. Therefore, at small particle densities, the mGW approach gives qualitatively the same quasi-momentum distribution as DMRG, i.e. the peaks locate at $k = 0$ and more bosons have negative momentum.

For the high density $n_0 = 1.25$ in figures 3(b) and (e), there exists more than one particle per site on average. Thus the vacuum state $|0\rangle$ is almost unoccupied in the ground state, i.e. $F_0^2 \ll F_2^2$. For $0 < \theta \leqslant \pi$, figure 3(b) clearly shows that the high peaks of the quasi-momentum distribution exactly appear at $k = -\theta$ in comparison with that at $k = 0$. The results of mGW qualitatively coincide with that of DMRG in figure 3(d) although the momentum value k of the DMRG peaks is a little larger than $-\theta$ because the peaks at $k = -\theta$ compete with the peaks at $k = 0$ under the influence of quantum fluctuation. Of course, $\theta = 0$ and $\theta = \pi$ still give the symmetric quasi-momentum distribution of bosonic operators.

Figures 3(c) and (f) show the quasi-momentum distribution at the density $n_0 = 0.75$ in the middle of $n_0 = 0.25$ and $n_0 = 1.25$. The competition between the $k = 0$ peak of the intensity A and the $k = -\theta$ of the intensity B of the quasi-momentum distribution leads to final peak shifts from $k = 0$ to the negative momentum but comes back to $k = 0$ while increasing θ from 0 to π as shown in figure 3(f). Note that this peculiar behavior is not reproduced by mGW in figure 3(c).

If we think about the occupation-dependent factor $e^{i\theta\hat{n}_j}$ in (4) again, we recognize in figure 3 a clear physical picture of the ground state: (i) for a small density $n_0 < 1$, the states $|0\rangle$ and $|1\rangle$ are preferred and $\Delta\beta_0 = 2m\pi$ is the leading term, which gives a quasi-momentum peak of bosons at $k \sim 0$; (ii) for a density $1 < n_0 < 2$, the states $|1\rangle$ and $|2\rangle$ are preferred and $\Delta\beta_1 = 2l\pi - \theta$ is the leading term, which gives a quasi-momentum peak of bosons at $k \sim -\theta$. In order to deal with the density $2 < n_0$, we should truncate the mGW approach at $n_{\max} = 3, 4, \cdots$. For example assuming $n_{\max} = 3$, the quasi-momentum distribution of bosons shows an additional peak of $k = -2\theta$. For the density $2 < n_0 < 3$, the leading peak of the quasi-momentum distribution of bosons appears at the momentum $k \sim -2\theta$.

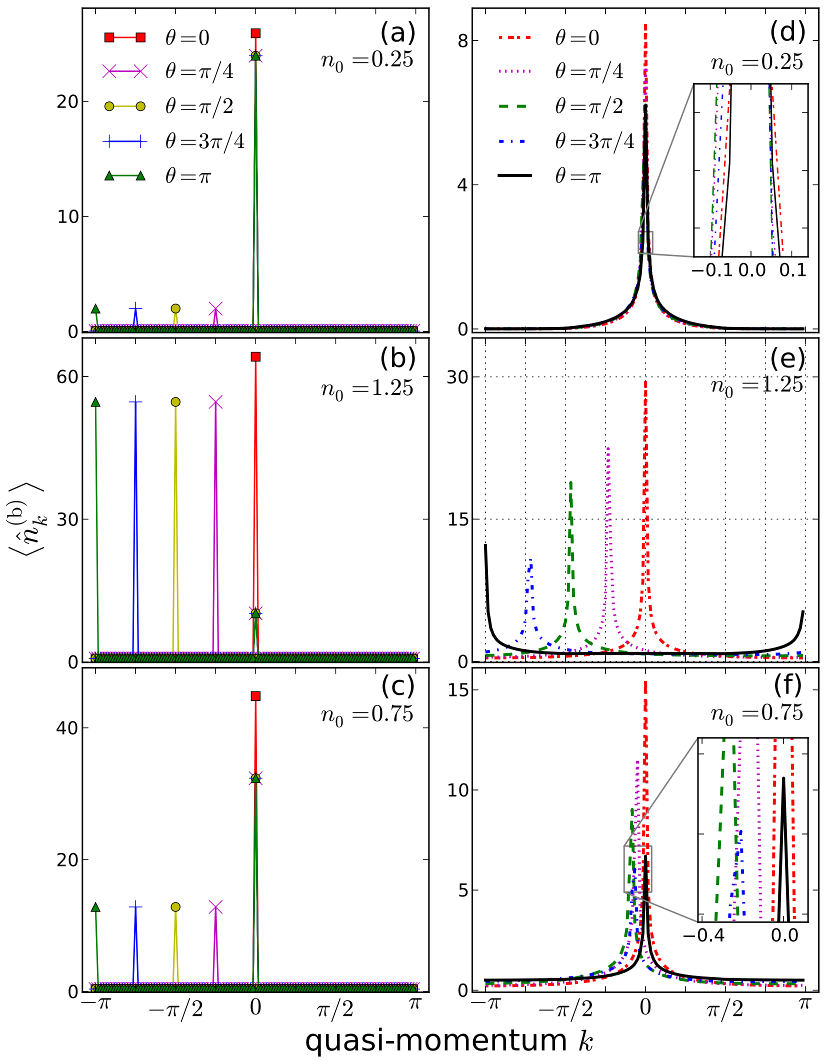

Figure 3. Quasi-momentum distribution of bosons with different statistical phase θ ($J/U = 0.1, L = 120$). (a)–(c) from mGW at density $n_0 = 0.25$, $n_0 = 1.25$, and $n_0 = 0.75$. (d)–(f) from DMRG at density $n_0 = 0.25$, $n_0 = 1.25$, and $n_0 = 0.75$.

5.2. Anyon quasi-momentum distribution

According to the equations (13) and (A.4) in the appendix, the anyonic correlation function is written as

$$\langle \hat{a}_i^\dagger \hat{a}_j \rangle \overset{i<j}{\rightarrow} \left[A + B\mathrm{e}^{\mathrm{i}(i-j+1)\theta}\right] \prod_{i<l<j} w, \tag{34a}$$

$$\langle \hat{a}_i^\dagger \hat{a}_j \rangle \overset{i>j}{\rightarrow} \left[A + B\mathrm{e}^{\mathrm{i}(i-j-1)\theta}\right] \prod_{j<l<i} w^*. \tag{34b}$$

where $w = F_0^2 + F_1^2 \mathrm{e}^{\mathrm{i}\theta} + F_2^2 \mathrm{e}^{\mathrm{i}2\theta} \equiv W\mathrm{e}^{\mathrm{i}\chi}$. If $\theta = 0$, we have $w = F_0^2 + F_1^2 + F_2^2 = 1$, otherwise the absolute value is $W < 1$. In the Bose limit $\theta = 0$, the correlation function of anyons is

$$\langle \hat{a}_i^\dagger \hat{a}_j \rangle = \delta_{ij} n_0 + \left(1 - \delta_{ij}\right) C. \tag{35}$$

Using equation (14b), the ground-state quasi-momentum distribution of anyons can be written as

$$\langle \hat{n}_k^{(a)} \rangle = n_0 - C + CL\delta_{k,0}. \tag{36}$$

If $\theta \neq 0$ and then $|w| < 1$, the quasi-momentum distribution of anyons is written as

$$\begin{aligned} \langle \hat{n}_k^{(a)} \rangle = n_0 &+ \frac{A}{L}\left[\mathrm{e}^{-\mathrm{i}k} \frac{(L-1) - Lu + u^L}{(1-u)^2} + \mathrm{c.c.}\right] \\ &+ \frac{B}{L}\left[\mathrm{e}^{-\mathrm{i}k} \frac{(L-1) - Lv + v^L}{(1-v)^2} + \mathrm{c.c.}\right], \end{aligned} \tag{37}$$

where $u = w\mathrm{e}^{-\mathrm{i}k}$ and $v = w\mathrm{e}^{-\mathrm{i}(k+\theta)}$. In the thermodynamic limit, this reduces to

$$\begin{aligned}\langle \hat{n}_k^{(a)} \rangle \underset{|w|<1}{\overset{L\to\infty}{\longrightarrow}} n_0 \quad &+ A\frac{2\cos k - 2W\cos\chi}{1 - 2W\cos(k-\chi) + W^2} \\ &+ B\frac{2\cos k - 2W\cos(\theta-\chi)}{1 - 2W\cos[(k+\theta)-\chi] + W^2},\end{aligned} \tag{38}$$

where $W = |w|$ and $\chi = \arg(w)$.

In the hard-core limit $F_2^2 = 0$, so we have $w = z$, $\chi = \varphi$, $A = n_0(1 - n_0)$, and $B = 0$, thus equation (38) reduces to equation (25). For small densities $n_0 \ll 1$, which implies $F_2^2 \sim 0$, we expect the quasi-momentum distribution of anyons in the soft-core case to be similar to that in the hard-core case. This can be shown by comparing figures 4 (a) and (b) from DMRG or (a′) and (b′) from mGW at the density $n_0 = 0.25$. However, for the fractional phase $\theta = \pi$ in the soft-case, we also note that there exists a quite small area with the property $\langle \hat{n}_k^{(a)} \rangle > 1$ that is shown as the shaded (yellow in color) zone in the insets of figures 4 (b) and (b′). The shaded area increases while increasing the density, for example $n_0 = 0.75$ is shown in figures 4 (d) and (d′). This result reveals that anyons with the statistical phase $\theta = \pi$ are pseudofermions, i.e. possibly more than one identical anyon exist in one state but they behave like a fermion while exchanging two anyons on different sites. Comparing the results from DMRG and mGW in figure 4, we demonstrate again that the mGW approach grasps the main features of the quasi-momentum distribution of anyons. Finally, we should note that the hard-core case is more suitable to describe the step-like behavior of anyons ($\theta = \pi$) than the soft-core case.

Figure 5 shows the fractional phase θ-dependence of anyonic $K_{\max}^{(a)}$ at the densities $n_0 = 0.25, 0.5, 1.25$, and 1.5. In general, for the density $0 < n_0 < 1$ and $0 < \theta < \pi$, $K_{\max}^{(a)}$ at density $n_0 = 0.5$ is larger than that at $n_0 = 0.25$, which coincides with the finding of the hard-core case. Moreover, for $1 < n_0 < 2$, the DMRG results show that the peak position $K_{\max}^{(a)}$ of the quasi-momentum distribution at density $n_0 = 1.25$ coincides with that at density $n_0 = 0.25$ within uncertainty. This is also shown by the DMRG results at density $n_0 = 1.5$ and $n_0 = 0.5$. However, the mGW approach in the thermodynamic limit shows that $K_{\max}^{(a)}$ at density $n_0 + 1$ is a little larger than that at density n_0, especially for the zone $\theta \sim \pi$.

6. Conclusions

In summary, we have studied the ground-state property of the 1D AH model. With the help of a fractional version of the Jordan–Wigner transformation, the AH model is mapped to the occupation-dependent hopping Bose–Hubbard model and, thus, the Hilbert space of anyons can be constructed from that of bosons. By calculating the two-point correlation function of creation and annihilation operators of bosons and anyons, we investigate the quasi-momentum distributions interpolating between Bose–Einstein statistics and Fermi–Dirac statistics. Theoretically, in order to include the influence of the fractional phase of anyons on the many-body wavefunction, we modify the classical Gutzwiller mean-field approach and get an analytic expression for the quasi-momentum distributions of anyons and bosons. In order to test the accuracy of the mGW mean-field approach, we use DMRG for numerical calculations.

In the hard-core case, the results show that the bosons condensate at zero momentum and have a symmetric quasi-momentum distribution around zero momentum. Due to the nonlocal string property, more anyons are shifted to a positive momentum and have an asymmetric quasi-momentum distribution, where the peak position depends on both the fractional phase and the particle number density. For the fractional phase $\pi/2 \leqslant \theta < \pi$, the GW approach yields an obvious smaller shift of positive momentum in comparison with the DMRG results.

In the soft-core case, the results show that the quasi-momentum peaks of bosons strongly depend on the particle number density. At density $n_0 < 1$, $\Delta\beta_0 = 2m\pi$ leads to a quasi-momentum peak of bosons at $k \sim 0$. However, mGW fails to reproduce the quasi-momentum distribution of bosons from DMRG at density $n_0 = 0.75$. At density $1 < n_0 < 2$, $\Delta\beta_1 = 2l\pi - \theta$ leads a quasi-momentum peak of bosons at $k \sim -\theta$. Again, the quasi-momentum distribution of anyons show nonlocal string behavior and yield similar features as in the hard-core case. Furthermore, anyons with $\theta = \pi$ are pseudofermions, i.e., there exists more than one identical anyon in one state in the soft-core case. However, in the hard-core case, the quasi-momentum distribution of anyons is a typical step-like function.

Acknowledgments

The authors would like to thank B Abdullaev, A Eckardt, S Hu, D Morath, M Roncaglia, I Schneider, S Srivastava, C Sträter, D Strassel, T Wang, and X-F Zhang for valuable discussions. This work was supported by Science Foundation of Heilongjiang (A201002), the Chinese Scholarship Council (CSC), the German Research

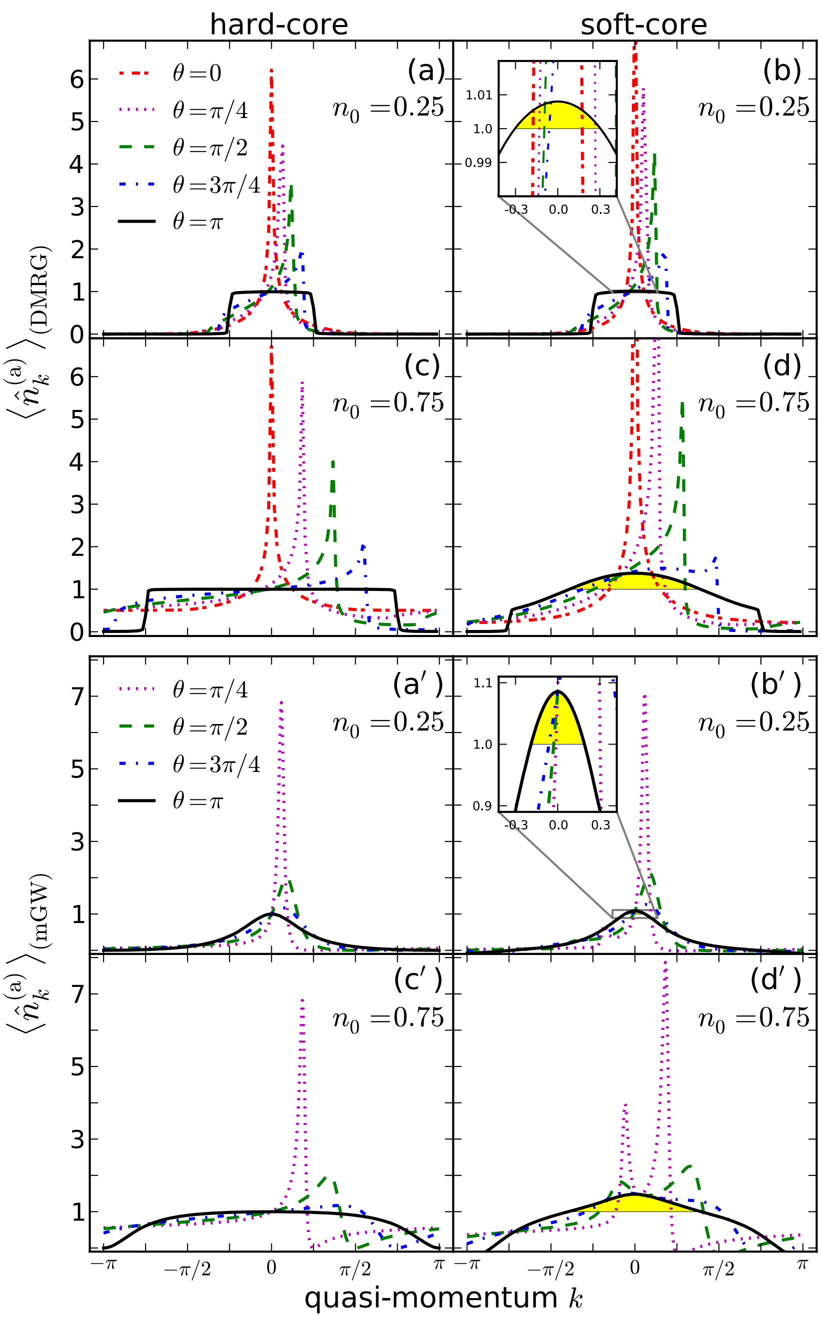

Figure 4. Quasi-momentum distribution of anyons with different statistical phase θ ($J/U = 0.1$). (a)–(d) from DMRG ($L = 120$) at density $n_0 = 0.25$ and $n_0 = 0.75$. (a′)–(d′) from mGW in the thermal dynamic limit at density $n_0 = 0.25$ and $n_0 = 0.75$. The left column (a), (c), (a′), (c′) and the right column (b), (d), (b′), (d′) refer to the hard-core case and the soft-core case, respectively.

Foundation (DFG) via the Collaborative Research Center SFB/TR49, and the Volkswagen Foundation via the German-Uzbek Project *Anyon Physics of Ultracold Atomic Gases*.

Appendix. Gutzwiller mean-field approach

Based on the Gutzwiller wave function (5), the interaction energy turns out to be

$$\begin{aligned}\mathcal{E}_{\text{int}} &= \sum_j \left\langle \Phi_j \middle| \frac{U}{2}\hat{n}_j\left(\hat{n}_j - 1\right) \middle| \Phi_j \right\rangle \\ &= \frac{U}{2}\sum_j\sum_{n=0}^{n_{\max}} \left|f_n^{(j)}\right|^2 n(n-1),\end{aligned} \tag{A.1}$$

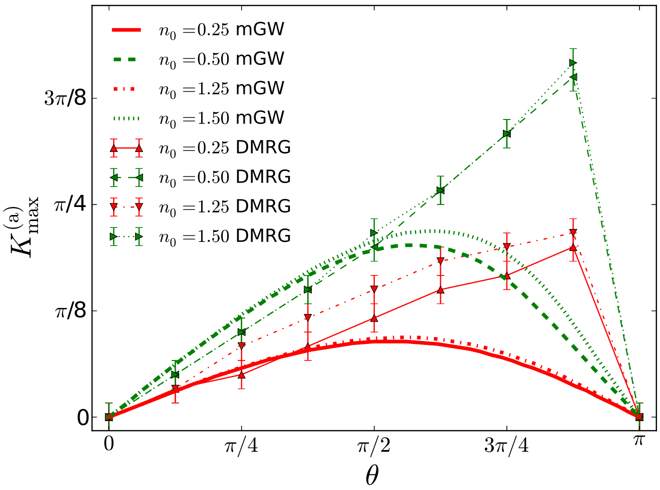

Figure 5. Quasi-momentum $K_{\max}^{(a)}$ plotted against the fractional phase θ of anyons resulting from DMRG ($L = 120$) and mGW (in the thermodynamic limit $L \to \infty$) with parameters $J/U = 0.1$, density $n_0 = 0.25,\ 0.5,\ 1.25$, and 1.5, respectively. The uncertainty of the quasi-momentum is of the order $\Delta k = 2\pi/L$.

whereas the chemical potential term within a grand-canonical description reads

$$\mathcal{E}_\mu = \sum_j \left\langle \Phi_j \middle| (-\mu)\hat{n}_j \middle| \Phi_j \right\rangle = -\mu \sum_j \sum_{n=0}^{n_{\max}} \left| f_n^{(j)} \right|^2 n. \tag{A.2}$$

In the same way, the expectation value of the kinetic energy term can be expressed as

$$\begin{aligned}\mathcal{E}_{\text{kin}} &= -J\sum_j \left(\left\langle \Phi_j \middle| \hat{b}_j^\dagger \mathrm{e}^{\mathrm{i}\theta\hat{n}_j} \middle| \Phi_j \right\rangle \left\langle \Phi_{j+1} \middle| \hat{b}_{j+1} \middle| \Phi_{j+1} \right\rangle + \text{c.c.} \right) \\ &= -J\sum_j \left(\left\langle \hat{b}_j^\dagger \mathrm{e}^{\mathrm{i}\theta\hat{n}_j} \right\rangle \left\langle \hat{b}_{j+1} \right\rangle + \text{c.c.} \right),\end{aligned} \tag{A.3}$$

where the expectation values $\langle \hat{O}_j \rangle \equiv \langle \Phi_j | \hat{O}_j | \Phi_j \rangle$ yield

$$\langle \hat{b}_j \rangle = \sum_{n=0}^{n_{\max}} f_n^{(j)*} f_{n+1}^{(j)} \sqrt{n+1} = \langle \hat{b}_j^\dagger \rangle^*, \tag{A.4a}$$

$$\langle \hat{b}_j^\dagger \mathrm{e}^{\mathrm{i}\theta\hat{n}_j} \rangle = \sum_{n=0}^{n_{\max}} f_n^{(j)} f_{n+1}^{(j)*} \sqrt{n+1}\, \mathrm{e}^{\mathrm{i}\theta n} = \langle \mathrm{e}^{-\mathrm{i}\theta\hat{n}_j} \hat{b}_j \rangle^*, \tag{A.4b}$$

$$\left\langle \hat{n}_j \right\rangle = \sum_{n=0}^{n_{\max}} \left| f_n^{(j)} \right|^2 n, \tag{A.4c}$$

$$\left\langle \mathrm{e}^{\pm\mathrm{i}\theta\hat{n}_j} \right\rangle = \sum_{n=0}^{n_{\max}} \left| f_n^{(j)} \right|^2 \mathrm{e}^{\pm\mathrm{i}\theta n}. \tag{A.4d}$$

Using equation (A.4), the Gutzwiller kinetic energy reduces to

$$\mathcal{E}_{\text{kin}} = -J \sum_j \sum_{m,n}^{n_{\max}} \sqrt{(n+1)(m+1)} \left[f_n^{(j)} f_{n+1}^{(j)*} f_m^{(j+1)*} f_{m+1}^{(j+1)} \mathrm{e}^{\mathrm{i}\theta n} + \text{c.c.} \right]. \tag{A.5}$$

Using the polar decomposition $f_n^{(j)} = F_n^{(j)} \mathrm{e}^{\mathrm{i}\alpha_n^{(j)}}$, we have

$$f_n^{(j)} f_{n+1}^{(j)*} f_m^{(j+1)*} f_{m+1}^{(j+1)} = F_n^{(j)} F_{n+1}^{(j)} F_m^{(j+1)} F_{m+1}^{(j+1)} \mathrm{e}^{\mathrm{i}\left[\beta_n^{(j)} - \beta_m^{(j+1)}\right]}, \tag{A.6}$$

where $\beta_n^{(j)} \equiv \alpha_n^{(j)} - \alpha_{n+1}^{(j)}$ denotes the difference between the phase of the probability amplitude $f_n^{(j)}$ of finding n bosons and $f_{n+1}^{(j)}$ of finding $n+1$ bosons on site j.

The ground state of the system with given parameters is determined from varying the coefficients $f_n^{(j)}$ and minimizing the total energy. This can either be done for a given chemical potential μ, or for a given mean particle number $n_0 = \langle \hat{n} \rangle = \sum_{n=0}^{n_{\max}} nF_n^2$ according to equation (A.4c). In this paper, we assume that n_0 is given, so the chemical potential $\mathcal{E}_\mu = -\mu n_0 L$ resulting from (A.2) does not depend on $f_n^{(j)}$. Thus, after having determined the Gutzwiller coefficients $f_n^{(j)}$, the chemical potential μ is fixed by

$$\mu = \frac{1}{L}\frac{\partial\left(\mathcal{E}_{\mathrm{int}} + \mathcal{E}_{\mathrm{kin}}\right)}{\partial n_0}. \tag{A.7}$$

A.1. Hard-core case

In the hard-core limit, bosons are impenetrable and each site contains at most one particle, i.e., $n_{\max} = 1$. In the GW approach, the normalization condition (6) reduces to $F_0^2 + F_1^2 = 1$. For a given particle number N, the mean density of particle number is given by $n_0 = N/L = F_1^2$ according to the equation (A.4*c*). Thus the absolute values of both Gutzwiller amplitudes are determined according to

$$F_0^2 = 1 - n_0, \quad F_1^2 = n_0. \tag{A.8}$$

The expectation value of the energy per lattice site $E_{\mathrm{tot}} = \mathcal{E}_{\mathrm{tot}}/L$ is then given by

$$\begin{aligned} E_{\mathrm{tot}}^{\mathrm{cGW}} &= -\mu n_0 - 2Jn_0\left(1 - n_0\right), \\ E_{\mathrm{tot}}^{\mathrm{mGW}} &= -\mu n_0 - 2Jn_0\left(1 - n_0\right)\cos\Delta\beta_0, \end{aligned} \tag{A.9}$$

where $E_{\mathrm{tot}}^{\mathrm{cGW}}$ and $E_{\mathrm{tot}}^{\mathrm{mGW}}$ refer to the cGW and mGW approach, respectively. The ground state is determined by minimizing the energy $E_{\mathrm{tot}}^{\mathrm{cGW}}$ and $E_{\mathrm{tot}}^{\mathrm{mGW}}$. This leads to

$$\Delta\beta_0 = 2m\pi, \tag{A.10}$$

where $m = 0, \pm 1, \pm 2, \cdots$. This expression shows that the mGW approach reduces to the cGW approach for hard-core anyons.

A.2. Soft-core case

Using the normalization condition (6) and equation (A.4*c*) in the GW approach, we have

$$\begin{aligned} F_0^2 + F_1^2 + F_2^2 &= 1, \\ F_1^2 + 2F_2^2 &= n_0, \end{aligned} \tag{A.11}$$

where we suppose $n_{\max} = 2$ as an approximation. The expectation value of the energy per lattice site reads now

$$\begin{aligned} E_{\mathrm{tot}}^{\mathrm{mGW}} = &-\mu n_0 + UF_2^2 - 2JF_1^2\left\{F_0^2\cos\left(\Delta\beta_0\right) + 2F_2^2\cos\left(\Delta\beta_1 + \theta\right)\right. \\ &\left. + 2\sqrt{2}F_0F_2\cos\left(\frac{\Delta\beta_0 + \Delta\beta_1 + \theta}{2}\right)\cos\left(\beta_0 - \beta_1 - \frac{\theta}{2}\right)\right\}. \end{aligned} \tag{A.12}$$

In order to minimize (A.12), we must choose for the respective phases

$$\begin{aligned} \Delta\beta_0 = 2m\pi, &\quad \Delta\beta_1 + \theta = 2l\pi, \\ \beta_0 - \beta_1 - \frac{\theta}{2} &= (m + l)\pi, \end{aligned} \tag{A.13}$$

where $m, l = 0, \pm 1, \pm 2, \cdots$. This demonstrates that the non-vanishing θ influences the phase of the many-body wavefunction. Taking into account equation (A.11), the ground state can be found by varying the Gutzwiller coefficients F_0, F_1, F_2 and minimizing the energy

$$E_{\mathrm{tot}}^{\mathrm{mGW}} = -\mu n_0 + UF_2^2 - 2JC, \tag{A.14}$$

where $C \equiv F_1^2(F_0^2 + 2\sqrt{2}F_0F_2 + 2F_2^2)$. Note that the resulting occupations F_0^2, F_1^2, and F_2^2 of the states $|0\rangle$, $|1\rangle$, and $|2\rangle$ are not affected by θ. Obviously, in the hard-core limit $J/U \to 0$, we reproduce $F_2 \to 0$. Thus, in that case equation (A.11) goes over to (A.8), so the calculation reproduces the hard-core case of the last section.

Furthermore, if we set $\Delta\beta_0 = 2m\pi$ and $\Delta\beta_1 = 2l\pi$ in equation (A.12), the mGW approach reduces to the cGW approach, for which the energy is

$$\begin{aligned} E_{\mathrm{tot}}^{\mathrm{cGW}} = &-\mu n_0 + UF_2^2 - 2JF_1^2\left\{F_0^2 + 2F_2^2\cos(\theta)\right. \\ &\left. + 2\sqrt{2}F_0F_2\cos\left(\frac{\theta}{2}\right)\cos\left(\beta_0 - \beta_1 - \frac{\theta}{2}\right)\right\}. \end{aligned} \tag{A.15}$$

Comparing equations (A.14) with (A.15), it is straightforward to conclude that $E_{\mathrm{tot}}^{\mathrm{mGW}} \leqslant E_{\mathrm{tot}}^{\mathrm{cGW}}$, which shows that the mGW approach is superior to the cGW approach. Therefore, we restrict ourselves to evaluate the mGW approach for the soft-core case.

References

[1] Wilczek F 1982 *Phys. Rev. Lett.* **48** 1144
[2] Wilczek F 1982 *Phys. Rev. Lett.* **49** 957
[3] Tsui D C, Stormer H L and Gossard A C 1982 *Phys. Rev. Lett.* **48** 1559
[4] Laughlin R B 1983 *Phys. Rev. Lett.* **50** 1395
[5] Wen X G 1990 *Phys. Rev.* B **41** 12838
[6] Kitaev A Y 2003 *Ann. Phys.* **303** 2
[7] Das S S, Freedman M and Nayak C 2005 *Phys. Rev. Lett.* **94** 166802
[8] Bonderson P, Kitaev A and Shtengel K 2006 *Phys. Rev. Lett.* **96** 016803
[9] Stern A and Halperin B 2006 *Phys. Rev. Lett.* **96** 016802
[10] Nayak C, Simon S H, Stern A, Freedman M and Das S S 2008 *Rev. Mod. Phys.* **80** 1083
[11] Alicea J, Oreg Y, Refael G, von Oppen F and Fisher M P A 2011 *Nat. Phys.* **7** 412
[12] Stern A and Lindner N H 2013 *Science* **339** 1179
[13] Matthews J C F *et al* 2013 *Sci. Rep.* **3** 1539
[14] Gentile G 1940 *Nuovo Cimento* **17** 493
[15] Gentile G 1942 *Nuovo Cimento* **19** 106
[16] Dutt R *et al* 1994 *Int. J. Mod. Phys.* A **9** 2687
[17] Biedenharn L C 1989 *J. Phys. A: Math. Gen.* **22** L873
[18] Macfarlane A J 1989 *J. Phys. A: Math. Gen.* **22** 4581
[19] Parthasarathy R and Vishwanathan K S 1991 *J. Phys. A: Math. Gen.* **24** 613
[20] Shen Y, Ai Q and Long G L 2010 *Physica* A **389** 1565
[21] Haldane F D M 1991 *Phys. Rev. Lett.* **67** 937
[22] Polychronakos A P 1996 *Phys. Lett.* B **365** 202
[23] Khare A 1990 *Fractional Statistics and Quantum Theory* 2nd Edn (Singapore: World Scientific)
[24] Vitoriano C and Coutinho-Filho M D 2009 *Phys. Rev. Lett.* **102** 146404
[25] Keilmann T, Lanzmich S, McCulloch L and Roncaglia M 2011 *Nat. Commun.* **2** 361
[26] Ma R, Tai M E, Preiss P M, Bakr W S, Simon J and Greiner M 2011 *Phys. Rev. Lett.* **107** 095301
[27] Greschner S and Santos L 2015 *Phys. Rev. Lett.* **115** 053002
[28] Sträter C, Srivastava S and Eckardt A in preparation
[29] Kundu A 1999 *Phys. Rev. Lett.* **83** 1275
[30] Batchelor M T, Guan X-W and Oelkers N 2006 *Phys. Rev. Lett.* **96** 210402
[31] Batchelor M T and Guan X-W 2006 *Phys. Rev.* B **74** 195121
[32] Batchelor M T, Guan X-W and He J-S 2007 *J. Stat. Mech.* P03007
[33] Hao Y, Zhang Y and Chen S 2008 *Phys. Rev.* A **78** 023631
[34] Santos R A, Paraan F N C and Korepin V E 2012 *Phys. Rev.* B **86** 045123
[35] Calabrese P and Mintchev M 2007 *Phys. Rev.* B **75** 233104
[36] Hao Y and Chen S 2012 *Phys. Rev.* A **86** 043631
[37] Wright T M, Rigol M, Davis M J and Kheruntsyan K V 2014 *Phys. Rev. Lett.* **113** 050601
[38] Wang L, Wang L and Zhang Y 2014 *Phys. Rev.* A **90** 063618
[39] Preiss P M, Ma R, Eric T M, Lukin A, Rispoli M, Zupancic P, Lahini Y, Islam R and Greiner M 2015 *Science* **347** 1229
[40] Longhi S and Valle G D 2012 *Phys. Rev.* B **85** 165144
[41] Hao Y, Zhang Y and Chen S 2009 *Phys. Rev.* A **79** 043633
[42] Rokhsar D S and Kotliar B G 1991 *Phys. Rev.* B **44** 10328
[43] Krauth W, Caffarel M and Bouchaud J P 1992 *Phys. Rev.* B **45** 3137
[44] Jaksch D, Bruder C, Cirac J I, Gardiner C W and Zoller P 1998 *Phys. Rev. Lett.* **81** 3108
[45] Schroll C, Marquardt F and Bruder C 2004 *Phys. Rev.* A **70** 053609
[46] White S R and Noack R M 1992 *Phys. Rev. Lett.* **68** 3487
[47] White S R 1992 *Phys. Rev. Lett.* **69** 2863
[48] Xie Z Y, Jiang H C, Chen Q N, Weng Z Y and Xiang T 2009 *Phys. Rev. Lett.* **103** 160601
[49] Hu S, Turner A M, Penc K and Pollmann F 2014 *Phys. Rev. Lett.* **113** 027202
[50] Hu S, Normand B, Wang X and Yu L 2011 *Phys. Rev.* B **84** 220402(R)
[51] Ostlund S and Rommer S 1995 *Phys. Rev. Lett.* **75** 3537
[52] Dukelsky J, Martn-Delgado M A, Nishino T and Sierra G 1998 *Europhys. Lett.* **43** 457
[53] Schollwöck U 2011 *Ann. Phys., NY* **326** 96
[54] Wall M L and Carr L D 2012 *New J. Phys.* **14** 125015
[55] Rossini D and Fazio R 2012 *New J. Phys.* **14** 065012
[56] Wall M L 2014 *computer code OPEN SOURCE MPS v1.0 Carr Theoretical Physics Research Group* (https://sourceforge.net/p/openmps/)